AUTHOR QUERY FORM

Please provide your responses and any corrections by annotating this PDF and uploading it according to the instructions provided in the proof notification email.

Dear Author,

Below are the queries associated with your article; please answer all of these queries before sending the proof back to AIP. Please indicate the following:

Figures that are to appear as color online only (i.e., Figs. 1, 2, 3) _____ (this is a free service).

Figures that are to appear as color online and color in print_____ (a fee of $325 per figure will apply).

Article checklist: In order to ensure greater accuracy, please check the following and make all necessary corrections before returning your proof.

1. Is the title of your article accurate and spelled correctly?

2. Are the author names in the proper order and spelled correctly?

3. Please check affiliations including spelling, completeness, and correct linking to authors.

4. Did you remember to include acknowledgment of funding, if required, and is it accurate?

Location in article	Query / Remark: click on the Q link to navigate to the appropriate spot in the proof. There, insert your comments as a PDF annotation.
AQ1	Please note that the term "magnetorresistance" has been changed to "magnetoresistance" throughout the text. Please check and confirm.
AQ2	In sentence beginning "We elaborate more on this," please verify that following section refers to Sec. III and IV
AQ3	Figures must be cited in numerical order; therefore, we have renumbered Figs. 6,7,8, and 9 as 7,8,9, and 6 Please check.
AQ4	Please provide page number for the Ref. 10.
AQ5	We were unable to locate a digital object identifier (doi) for Ref(s) 3, 4, 8, 15 and 20. Please verify and correct author names and journal details (journal title, volume number, page number, and year) as needed and provide the doi. If a doi is not available, no other information is needed from you. For additional information on doi's, please select this link: http://www.doi.org/.

Thank you for your assistance.

On the origin of the low temperatures resistivity minimum in Cr thin films

E. Osquiguil, L. Tosi, E. E. Kaul, and C. A. Balseiro

Centro Atómico Bariloche and Instituto Balseiro, Comisión Nacional de Energía Atómica, 8400 Bariloche, Argentina

We present measurements of the electrical resistivity and Hall coefficient, ρ and R_H, in Cr films of different thicknesses grown on MgO (100) substrates, as a function of temperature T and applied magnetic field H. The results show a low temperature minimum in $\rho(T)$, which is thickness dependent. From 40 K to 2 K, the Hall coefficient is a monotonous increasing function as T is reduced with no particular signature at the temperature T_{min} where the minimum develops. We explain the resistivity minimum assuming an imperfect nesting of the Fermi surface leading to small electron and hole pockets. We introduce a phenomenological model which supports this simple physical picture. © 2013 AIP Publishing LLC. [http://dx.doi.org/10.1063/1.4846757]

I. INTRODUCTION

Chromium metal is the only simple metal showing itinerant antiferromagnetism at room temperature. After the seminal works by Overhauser in the early 1960s,[1] Cr has been recognized as the paradigmatic case of density waves instabilities, a macroscopic manifestation of collective quantum states of the charged electrons in metals.

The stability and structure of the spin density wave (SDW) state in metals depends crucially on the nesting properties of the Fermi surface (FS). SDW states occur when the FS of the interacting electrons present large parallel regions spanned by a nesting wave vector Q. The condensation of a SDW, a broken symmetry state with long range magnetic correlations modulated by the wave vector Q, is accompanied by the destruction of part of the FS or, for good nesting or large enough SDW amplitudes, the development of a semiconductor gap in the spectrum. Consequently, the transport properties are sensitive to the occurrence of the SDW showing either an increase of the resistivity $\rho(T)$ and changes in the Hall resistance at the transition temperature T_N or a real metal-insulator transition for good FS nesting.

In Cr single crystals, the SDW is characterized by wave vectors $Q_{\pm} = (2\pi/a_{Cr})(1\pm\delta)$ along the $\langle 100 \rangle$ directions, $a_{Cr} = 2.88$ Å is the lattice parameter of the Cr bcc unit cell at room temperature, and δ is the deviation from commensurability. The resistivity $\rho(T)$ shows an increase at the transition temperature $T_N = 311$ K, an effect that together with the behaviour of the Hall resistance suggests the partial destruction of the FS at the onset of the SDW leading to the formation of small electron and hole pockets.[2] Notably, in dirty samples, a low temperature minimum is observed in $\rho(T)$. The first systematic studies of the resistivity minimum in the incommensurate-SDW phase of Cr were done by Semenenko.[3] In these studies, it was shown that in several Cr samples with different unknown levels of impurities, the temperature of the minimum in $\rho(T)$ increased rather sharply as the residual resistivity of the sample increased. It was then found that bulk Cr samples with small amounts of Fe produced not only a minimum in $\rho(T)$ but also changed the Néel temperature and the resistivity behavior below it.[4,5]

Triggered by these works, Arajs and coworkers extended the study of the resistivity behavior at low temperatures of binary Cr alloys with small and varying atomic quantities of different solutes[6,7] such as Fe, Ni, Co, Mn, Ge, and Si. Although the minimum in $\rho(T)$ was observed in all but Mn alloys, an interpretation in terms of a Kondo-like scattering of the conduction electrons could not account for their data, in particular, the disagreement observed for the solute concentration dependence of the minimum temperature and the lack of Curie-Weiss paramagnetic response in the SDW state.

The disagreement of these and other experimental results in Cr binary and ternary alloys with the Kondo model led Volkov and Tugushev to introduce a theoretical model Resonant Impurity Scattering(RIS) based on the formation of local impurity states in systems with a SDW ground state.[8–11] They predicted that under certain conditions, nonmagnetic impurities may generate spin-polarized states within the SDW gap. The interaction of electrons with these localized states could produce an increasing resistivity when lowering T, which combined with the electron-phonon temperature dependence for the scattering time may give rise to a minimum in $\rho(T)$. The model also predicts a negative magnetoresistance at low temperatures. It has been speculated that within this scenario, a wealth of experimental data in Cr binary and/or ternary alloys with varying solute concentrations may be explained.[12]

During the last decade, the advances in spintronics renewed the interest in Cr base materials including superlattices and thin films.[13–20] The resistivity minimum has also been observed in Cr thin films prepared by different growing methods.[21] In thin films, the three crystallographic directions become non-equivalent as the film thickness decreases and the wave vector Q orients perpendicular to the film surface. The critical temperature T_N decreases, and the SDW are transverse, with the spin perpendicular to the wave vector Q, down to the lowest studied temperatures. Boundary conditions at the film surfaces leads to the quantization of the wave vector Q, giving rise to very interesting phenomena.[22–24] In these films, the residual resistivity is in general quite large, increasing as the film thickness decreases

AQ1

95 due to crystallographic defects induced at the sample sub-
96 strate interface. Despite of the different nature of the defects
97 in films and in impurity-doped crystals, and due to the lack
98 of a universal—independent of the defect nature—theory,
99 the RIS model has been recently used to analyse the mini-
100 mum in $\rho(T)$ observed in some films.

101 In this paper, we explore the low temperature and mag-
102 netic field dependence of the transport properties of Cr films.
103 We present a systematic study of samples of different thick-
104 nesses prepared following the same procedure. We show that
105 the observed resistivity minimum can be explained using a
106 general model that does not rely on the specific nature of the
107 defects. We argue that it suffices to assume an imperfect
108 nesting of the hole and electron sheets of the FS and a gen-
109 eral electron-phonon scattering to account for our experi-
110 mental results: the minima in $\rho(T)$. We also discuss its
111 evolution with magnetic field, and the positive magnetore-
112 sistance. We argue that the same mechanism can also explain
113 the low temperature resistivity of other systems containing
114 spin or charge density waves.

II. EXPERIMENTAL RESULTS AND DISCUSSION

A. The samples

117 Cr thin films were grown on MgO (100) substrates using
118 DC Magnetron Sputtering in a similar way as that reported
119 by Kummamuru *et al.*[22] using a unique 99.99% pure Cr tar-
120 get. The films, with thicknesses between 10 nm and 350 nm,
121 were characterized by x-ray diffraction showing rocking
122 curves that have an angular dispersion at FWHM around the
123 [002] peak of $0.5°$, indicating a preferred orientation in the
124 (100) direction. Results from AFM scans show a mean sur-
125 face roughness of about 2 nm, which is the third part of the
126 SDW wavelength Λ_{SDW} at low temperatures. The samples
127 were patterned in a six terminal configuration bar of 2 mm
128 long and 140 μm wide using photolithography and chemical
129 etching. The resistance was measured using a dc current of
130 10 μA as a function of T in steps of 0.5 K: between 20 K and
131 320 K in a commercial cryo-cooler and between 2 K and
132 40 K in an Oxford 18 T Teslatron. Hall measurements
133 between 2 K and 40 K were performed in an Oxford 18 T
134 Teslatron system following the field inversion method.

B. The low temperature resistivity

136 In the upper panel of Fig. 1, we show the resistivity $\rho(T)$
137 for films with different thicknesses at zero magnetic field. As
138 can be seen, the resistivity increases as the film thickness is
139 reduced. In order to quantify this, in the inset, we show
140 $\rho(4 \text{K})$ as a function of L. Unlike the results of Ref. 21, all
141 samples were prepared following the same procedure and
142 with the same Cr target. Therefore, it is reasonable to assume
143 that the type of defects and impurities are the same in all
144 films. Those defects are structural defects mainly due to, or
145 generated by, the mismatch between the lattice constant of
146 Cr and MgO substrate. However, as it is well known, the
147 relative importance of such defects to determine the residual
148 resistivity increases as the film thickness is decreased. An
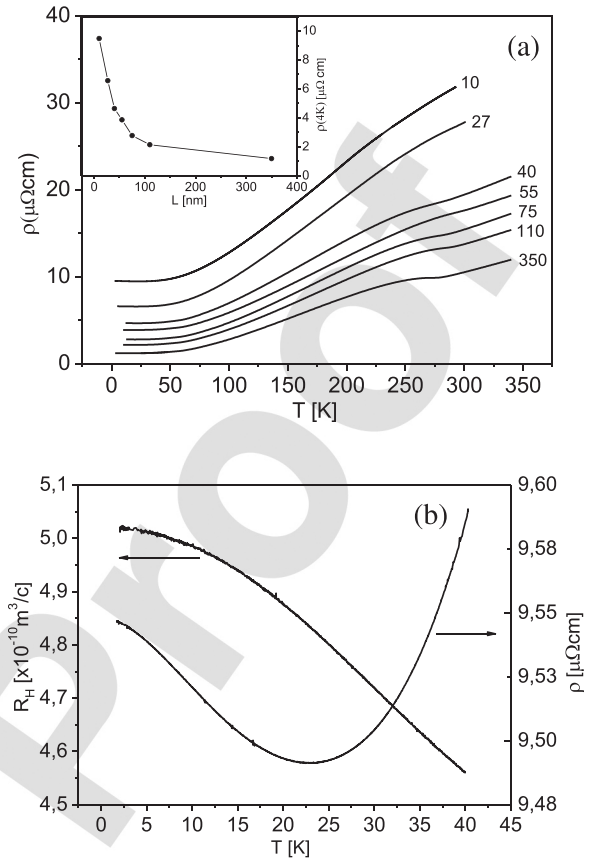149 important feature of the results in Fig. 1 upper panel that

FIG. 1. (a) Resistivity of the films as a function of temperature for different thicknesses L. The label near each curve corresponds to the thickness expressed in nm. The inset shows the resistivity at 4 K as a function of L. (b) Resistivity $\rho(T)$ at $H = 0$ and Hall coefficient $R_H(T)$ for the 10 nm thick film at $H = 12$ T.

150 cannot be observed due to the scale is the existence of a min-
151 imum in $\rho(T)$ at low temperatures for all measured samples.

152 This is shown in Fig. 1 lower panel for the thinnest film
153 $(L = 10 \text{ nm})$. The figure also shows the behaviour of the Hall
154 coefficient $R_H(T)$ measured at $H = 12$ T in the same tempera-
155 ture window where the minimum displays. Two interesting
156 features should be noted: (i) the amplitude of the minimum
157 defined as $\rho(4 \text{ K}) - \rho(T_{min})$ is two orders of magnitude
158 smaller than $\rho(T_{min})$, and (ii) the Hall coefficient is a monot-
159 onous decreasing function of temperature, showing no sign
160 of the minimum displayed by $\rho(T)$. Both features are shared
161 by all measured films.

162 The low temperature resistivity for films of different
163 thicknesses is shown in Fig. 2. In order to compare the differ-
164 ent curves, the residual resistivity ρ_0 of each sample has
165 been subtracted. As can be observed, the minimum shifts to
166 lower temperatures and its amplitude decreases as the film
167 thickness increases. The continuous lines are fittings using
168 the expression $\rho(T) = \rho_0(1 + AT^3)/(1 + BT^2)$ as discussed
169 below.

170 In the upper panel of Fig. 3, we plot the temperature at
171 which the minimum in $\rho(T)$ occurs as a function of the film
172 thickness L. The solid line in the main panel is a guide to the
173 eye. Notably, T_{min} increases sharply as L is reduced. In the
174 inset, we show that this increase follows a power law.
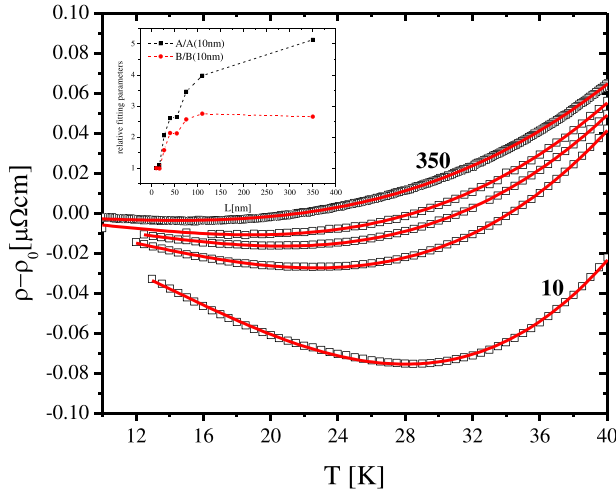175 Although we do not have an explanation for this particular

FIG. 2. Low temperature resistivity difference $\rho(T) - \rho_0$ for films of different thicknesses L. The curves correspond to films of $L = 10$, 40, 75, 110, and 350 nm from bottom to top. The inset shows the normalized parameters A and B used in the fitting (see text).

thickness dependence, what is interesting to note is that an increase in the residual resistivity $\rho(4\,K)$ is accompanied by an increase in the temperature where the minimum occurs. This is clearly observed in a plot like that shown in the lower panel of Fig. 3. If we interpret $\rho(4\,K)$ as a measure of the disorder present in each film, then an increase in the film's

structural disorder shifts resistivity minimum to higher temperatures and increases the residual resistivity shifting the $\rho(T)$ curves to higher values. These data display a similar behavior as those shown in Fig. 2 of Ref. 3. We believe that this is not a fortuitous coincidence but a clear sign that the origin of the resistivity minima in Cr samples with small amounts of non-magnetic impurities is more universal than previously thought,[8] and that it should have an explanation independent of the type of impurity that is added to Cr.

C. The magnetoresistance

A new insight on the minima's origin may be obtained by looking on the effects of applying a magnetic field H to the films. We present the results for a 10 nm thick film, measurements performed in a film one order of magnitude thicker show similar behaviors. First we note that, within experimental error, no longitudinal magnetoresistance was observed for fields parallel to the films. For transverse fields two new features appear: (i) a *positive* magnetoresistance for temperatures above and below T_{min} which follows an H^2 behavior up to $\sim 12\,T$ with a tendency to saturation at higher magnetic fields as seen in Fig. 4 upper panel, and (ii) although the amplitude of the minimum $\Delta\rho = \rho(T_{min}) - \rho(2\,K)$ is reduced by approximately 80% *the minimum is not suppressed by fields up to* 16 T, as clearly illustrated in Fig. 4 lower panel. Both results points against an interpretation of the minima as due to the existence of magnetic
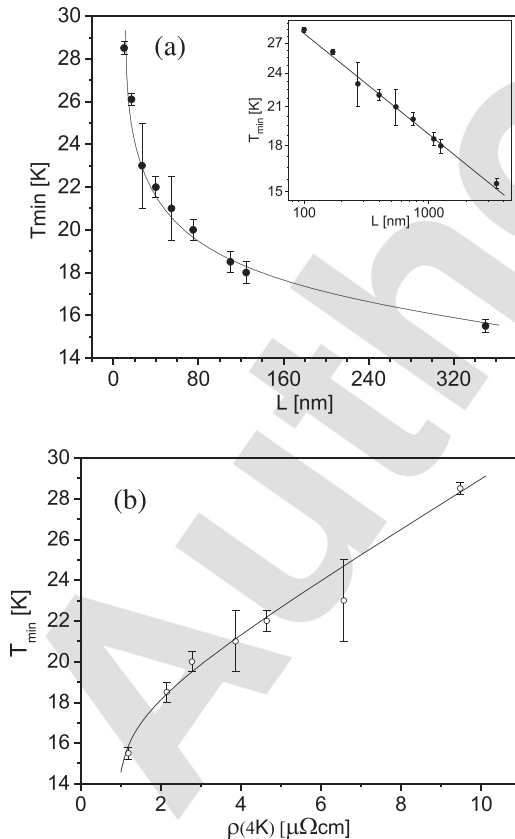

FIG. 3. (a) Temperature at which the resistivity is minimum T_{min} as a function of film thickness. The solid line is a guide to the eye. The inset shows that $T_{min}(L)$ follows a power law (see text). (b) Temperature of the minimum resistivity as a function of the residual resistivity. The solid line is a guide to the eye.
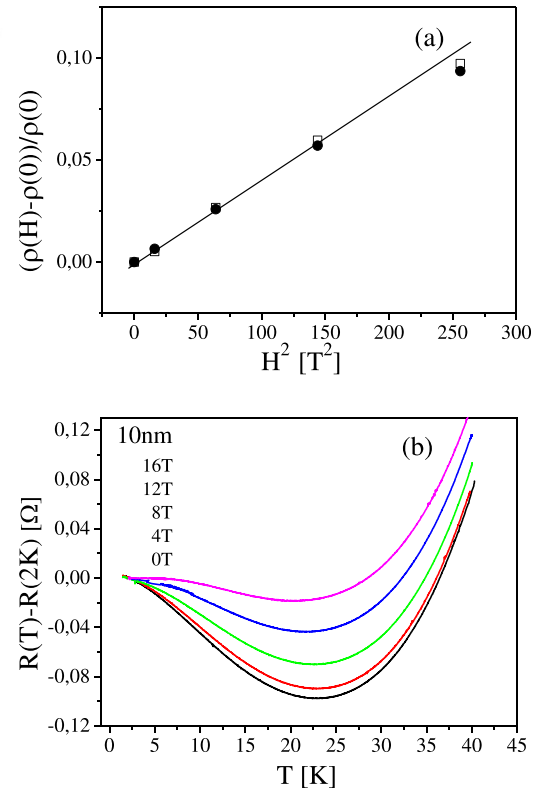

FIG. 4. (a) Magnetoresistance for two temperatures (5 K squares, 35 K circles), as a function of the square of the applied magnetic field. The solid line is a guide to the eye. (b) Resistivity minimum for the 10 nm thick film for increasing applied magnetic fields. In order to appreciate the whole variation of $\rho(T, H)$, we have subtracted the value $\rho(2\,K)$ in each curve.

impurities giving rise to a Kondo-like or RIS mechanism. We elaborate more on this point in Secs. III and IV.

D. Discussion of the experimental results

There are two main effects that may generate a minimum in $\rho(T)$: a reduction of the carrier density n as T is reduced, or the appearance of a new scattering mechanism with a characteristic energy scale of the order of $k_B T_{min}$. In simple metals, n hardly changes with T, and therefore, if a minimum is observed in $\rho(T)$, it is probably due to a scattering process that turns on at or near the temperature of the minimum. This is in fact the case of the Kondo effect[25,26] and, as mentioned above, of the RIS model developed to explain the minima in $\rho(T)$ of different Cr samples.[21] As for the Kondo effect, a *negative* magnetoresistance is also expected in the RIS model.[8]

In what follows we give a plausibility argument suggesting that the possibility of having a new scattering mechanism responsible of the minimum in $\rho(T)$ of Cr may be ruled out whatever the origin of this new process might be.

In a simple one band metal, the ratio between the resistivity and the Hall coefficient $r = \rho(T)/R_H$ is a quantity that depends on the relaxation time $\tau(T)$ and is independent on the carrier density n, i.e., $r \propto 1/\tau(T)$. In such a metal, it is expected that if a new scattering (*ns*) mechanism turns on, or becomes relevant, at a certain temperature T_{ns}, r should increase when the temperature drops below T_{ns}. Indeed, because of Matthiessen's rule, the effective relaxation rate becomes $1/\tau_{eff}(T) = 1/\tau(T) + 1/\tau_{ns}(T)$, and the resistivity should grow below T_{ns}. The same type of argument can be applied to a compensated two band metal, as is the case with Cr. It is easy to show that $r(T)$ again is a function solely of the electron and hole effective masses, and the electron and hole relaxation times, but is independent of the carrier density $n = n_h = n_e$. Moreover, even if $n_e \neq n_h$ with a temperature independent ratio n_e/n_h, the same argument holds.[27] Therefore, in all these cases, a reduction of either the hole τ_h or electron τ_e scattering time (or both), due to the development of a new scattering process at a certain temperature, will give rise to an increase of the ratio $r(T)$.

In panel (a) of Fig. 5, we show the Hall coefficient for a 10 nm thick film in the temperature window where the minimum in $\rho(T)$ displays, measured at different magnetic fields. The first characteristic we may see is that, as anticipated in the lower panel of Fig. 1, the temperature dependence of R_H has no particular feature at T_{min}. The second result is that the Hall coefficient is not linear in H in this temperature window

($R_H(H)$ is linear in H at 150 K and 310 K). Non-linearities in $R_H(H)$ at 4.2 K have also been observed in some dilute Ti alloys whose resistivity show a minimum at low temperatures.[28] In our case, $R_H(H)$ decreases monotonously with increasing temperature.

In panel (b) of Fig. 5, we plot the ratio r as a function of temperature. Note that for the purpose of showing its temperature dependence, it is irrelevant to plot $\rho(T)/R_H(T)$ or $R(T)/R_H(T)$. Each resistance curve has been measured at the same magnetic field as the Hall coefficient.

As can be easily seen, r is a smooth increasing function of T with no trace of the minimum observed in $\rho(T)$ in the whole temperature range. This result, based on the plausibility argument presented above, also indicates that the minima in $\rho(T)$ may not be due to the appearance of a new scattering mechanism. Altogether these results are consistent with a change in the carrier density as the temperature is varied at low temperatures, an effect that should be expected in systems with small and temperature dependent electron and hole pockets.

In Sec. III, we show that our results can be consistently explained by assuming a mechanism that is related to an imperfect nesting of the FS and the occurrence of the SDW. As we show below, this produces a power law increase of $n(T)$ as T is increased, an effect that is combined with a reasonable assumption for the scattering rate of the carriers makes it possible to reproduce the behavior of $\rho(T)$, the evolution of the minimum as the magnetic field is varied and the positive magnetoresistance.

III. MODEL

In this section, we give a qualitative description of the SDW state in a system with no perfect nesting of the FS.[29,30] The following discussion aims to give a simple picture of the effect of partial nesting of the FS and is not based on the particular electronic structure of Cr. The model includes an electron and a hole bands described by the following Hamiltonian: $H = H_0 + H'$, where

$$H_0 = \sum_{k,\sigma} (\varepsilon_{1,k} c_{1,k\sigma}^\dagger c_{1,k\sigma} + \varepsilon_{2,k} c_{2,k\sigma}^\dagger c_{2,k\sigma}),$$

with $\varepsilon_{1,k} = -D_e + \hbar^2(k_x^2/2m_x^e + k_y^2/2m_y^e + k_z^2/2m_z^e)$ and $\varepsilon_{2,k} = D_h - \hbar^2(k_x^2/2m_x^h + k_y^2/2m_y^h + (k_z - Q)^2/2m_z^h)$. Energies are measured from the Fermi energy ($E_F = 0$). The SDW breaks the translational symmetry mixing the two bands, and thus, at the mean field level, the Hamiltonian H' is given by

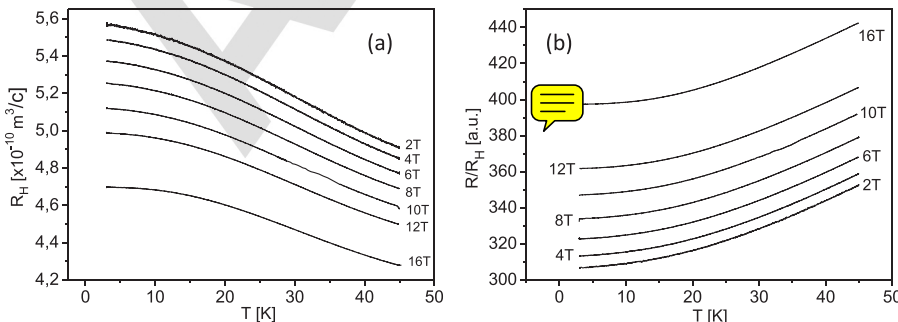
FIG. 5. (a) Hall coefficient as a function of temperature for different applied magnetic fields H. (b) Ratio $r = R(T)/R_H(T)$ for different applied magnetic fields. For both panels the label near each curve denotes H in Tesla.
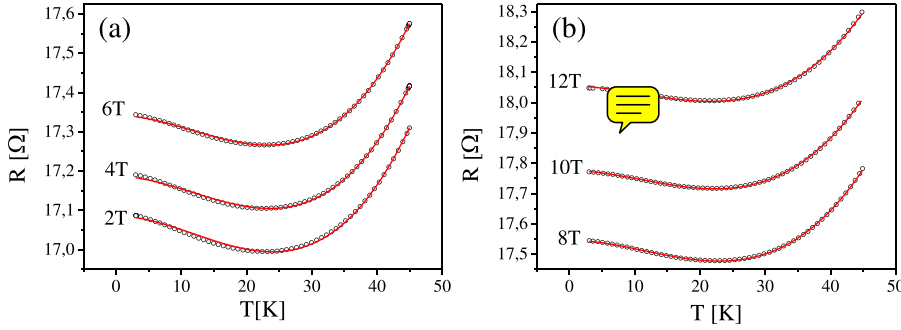
FIG. 6. Schematic representation of (a) the band structure and (b) the Fermi surface for electron and hole bands (as given in Eq. (1)) projected on the $k_z = 0$ plane resulting from an imperfect nesting. (c) Δ as function of temperature T and imperfect nesting coefficient γ. (d) Fermi surface for electron and hole bands with different volumes in reciprocal space as in the case of Cr metal

$$H' = \Delta \sum_{k,\sigma} \sigma(c^{\dagger}_{1,k\sigma} c_{2,k+Q\sigma} + h.c.),$$

where Δ is the SDW order parameter of wave vector Q and is given by the solution of the following equation:

$$1 = -\frac{V}{(2\pi)^3} \int_0^{k_{max}} \frac{f(E_k^+) - f(E_k^-)}{E_k^+ - E_k^-} dk^3,$$

where V is an effective interaction, k_{max} a momentum cutoff, $f(E)$ is the Fermi function, and

$$E_k^{\pm} = \frac{\varepsilon_{1,k} + \varepsilon_{2,k+Q}}{2} \pm \sqrt{\left(\frac{\varepsilon_{1,k} - \varepsilon_{2,k+Q}}{2}\right)^2 + \Delta^2}.$$

In order to minimize the number of independent parameters of the model, we take

$$\begin{aligned}
\varepsilon_{1,k} &= -D + \frac{\hbar^2}{2m^*}((1+\gamma)k_x^2 + (1-\gamma)k_y^2 + k_z^2), \\
\varepsilon_{2,k+Q} &= D - \frac{\hbar^2}{2m^*}((1-\gamma)k_x^2 + (1+\gamma)k_y^2 + k_z^2),
\end{aligned} \tag{1}$$

where γ measures the lack of nesting of the electron and hole Fermi surfaces. Fig. 6 shows a schematic representation of the band structure and the behavior of the SDW order parameter in the (T, γ) plane. Fig. 7 shows the density of states

(DS) for different values of the nesting parameter γ. For simplicity, we have chosen to preserve the electron-hole symmetry, an extension to a more general case is straightforward.

This simple model, which captures the essential aspects of the conventional SDW theory, illustrates what are the main consequences of the lack of nesting (γ): (i) for sufficiently large γ, the DOS develops a pseudogap rather than a real gap, and (ii) at low temperatures, the mean field order parameter Δ shows a power law temperature dependence rather than an exponential one. The structure of the DS shown in the Fig. 7, with the characteristic van Hove singularities and a gap that closes as the nesting is reduced, is a general result that depends only on the nesting properties of the FS and not on the details of the electronic structure. In Cr, the two pieces of the Fermi surface have different volumes as schematically shown in Fig. 6(d), and the DOS for a given Δ shows a pseudogap with the Fermi energy shifted from the minimum.

In summary, in Cr single crystal and in Cr films, the Fermi energy in the SDW phase lies in a pseudogap with small electron and hole pockets. First principles band structure calculations in the SDW phase of Cr show the occurrence of the pseudogap.[31,32] The total number of electrons in the conduction band is given by

$$n_c(T) = \frac{1}{(2\pi)^3} \int_0^{k_{max}} f(E_k^+) dk^3 = \int D_c(\varepsilon) f(\varepsilon) d\varepsilon, \tag{2}$$

where $D_c(E)$ is the density of states of the conduction band. The low temperature behaviour of the carrier density changes from exponential for the semiconducting case to a power-law behaviour, $n(T) \simeq n_0(1 + BT^2)$, for the gapless situation. This temperature dependence of the carrier density is central to the behaviour of the resistivity. To show this, let us first consider the simplest description: using the Drude formula for the conductivity we get $\sigma^c(T) = n_c(T)e^2\tau(T)/m^*$ for the contribution of the conduction band, a similar expression gives the contribution of the valence band. The temperature dependence of the relaxation (scattering) time is due to the electron-phonon interaction, which in simple metals gives $1/\tau(T) = 1/\tau_0 + \lambda T^m$ with $m = 5$. However, in transition metals, the exponent m changes due to interband transitions or due to the presence of disorder[33] and in what follows we take the value $m = 3$ that is often observed in these materials. Combining these temperature dependent quantities, the resistivity can be written as
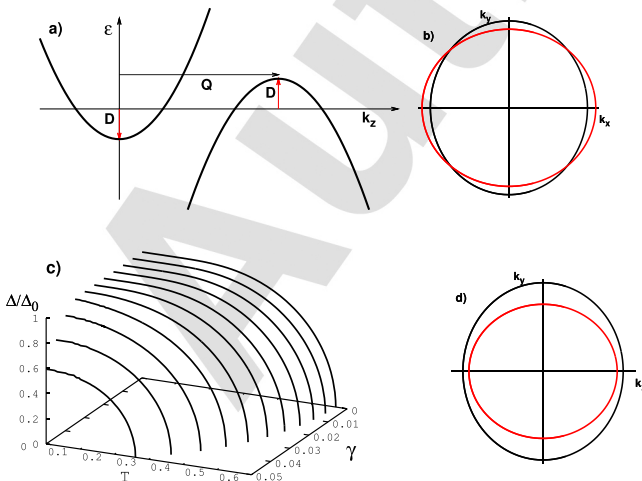

FIG. 7. Density of states arising from the model with (a) $\gamma = 0$, (b) $\gamma = 0.02$, and (c) $\gamma = 0.04$ showing a finite value at the Fermi level for imperfect-enough nesting.

$$\rho(T) = \rho_0 \frac{(1 + AT^3)}{(1 + BT^2)}. \tag{3}$$

In the above equation, the constant $A = \tau_0 \lambda$ measures the ratio of the electron-phonon and the impurity contributions to the resistivity. The largest the residual resistivity the smaller the value of A. The parameter B can be estimated using the Sommerfeld expansion to evaluate the integral of Eq. (2) with an approximate DOS of the form (see Fig. 7) $D_c(\varepsilon) = \gamma \sqrt{\varepsilon_0 + \varepsilon}$ giving $B = \pi^2 k_B^2 / 8\varepsilon_0^2$. For a very rough estimation, taking ε_0 of the order of Δ, which in turn is of the order of the critical temperature T_N, we finally get a value for $B \sim 10^{-5}\,\mathrm{K}^{-2}$, which is in good agreement with the values used to fit the experimental curves (see below).

To be more precise, we calculate the conductivity using Kubo formula. For the conduction band we have

$$\sigma_{xx}^{(c)} = \frac{e^2}{(2\pi)^3} \int_0^{k_{\max}} \left(-\frac{\partial f(E_k^+)}{\partial E_k^+} \right) (v_x^+(k))^2 \tau(k) dk^3,$$

where $v_x^+(k) = (1/\hbar)\partial E_k^+/\partial k_x$. Summing the contributions from the conduction and valence bands and assuming a k-independent relaxation time $\tau \equiv \tau(k)$, we numerically evaluate the integrals obtaining, as expected, a low temperature dependence of the form $C\tau(1 + \tilde{B}T^2)$ with a new coefficients $\tilde{B}$ and C. This is shown in Fig. 8. The values of $\tilde{B}$ are similar to the ones obtained in the calculation of the carrier density.

In Figs. 2 and 9 we show the fits of the resistivity data with Eq. (3). A very good agreement with the model prediction can be observed.

IV. DISCUSSION AND CONCLUSIONS

The above discussion suggests that in the case of imperfect nesting of the FS, the low temperature resistivity of the SDW phase is given by $\rho(T)/\rho_0 = (1 + AT^3)/(1 + BT^2)$. Here the numerator comes from the temperature dependence of the relaxation time τ characteristic of transition metals and the coefficient A decreases as the residual resistivity increases. The denominator is due to the temperature change of the carrier density, and the coefficient B is determined by the nesting properties of the FS. The magnitude of A is of the order of that used in Ref. 21, while a rough estimation of B is in good agreement with values used in the fittings of the experimental curves.

An important point concerns the variation of the fitting parameters with the film thickness. As the thickness decreases, we expect the residual resistivity to increases due to the relative importance of the structural defects induced by the film-substrate mismatch (see inset of Fig. 1). This increase should be reflected in a decrease of the parameter A. At the same time, except for very thin films where the stress can affect the electronic structure and consequently the SDW structure, we expect the number of carriers and its temperature dependence (the parameter B) to be thickness independent. This is precisely what is observed in a wide range of thicknesses (see inset of Fig. 2). Only for the thinner films ($L \lesssim 50\,\mathrm{nm}$), we observe small variations in the parameter B.
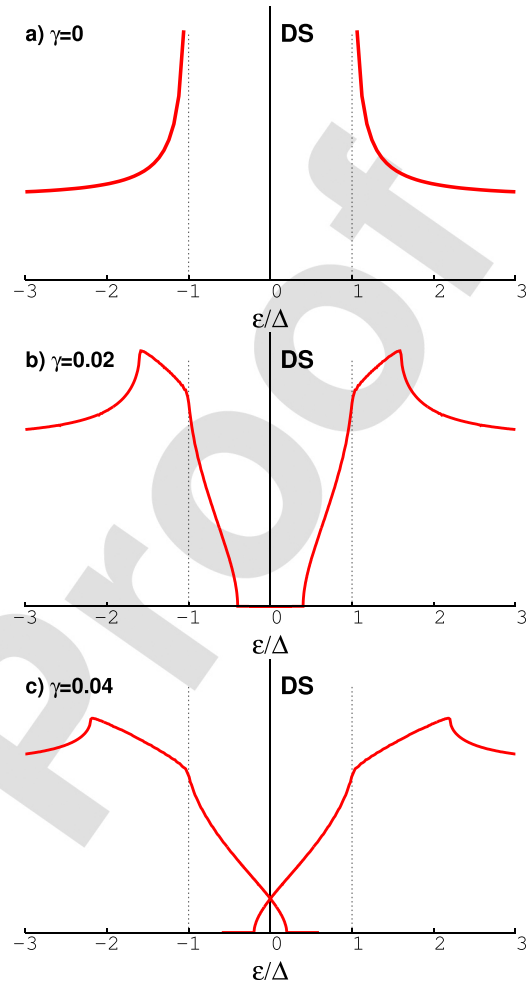

FIG. 8. Conductivity divided by relaxation time as a function of temperature calculated from the model using Kubo formula.

Concerning the magnetic field effect on the transport properties, we observe a small anomalous positive magnetoresistance following a H^2 behaviour for temperatures above and below T_{min}. The temperature of the minimum T_{min} is weakly dependent on H although the amplitude of the minimum $\Delta\rho$ is reduced but not suppressed by fields up to 16 T. The effect of external magnetic fields on the SDW structure, and consequently on the particular features of the magneto-transport properties, is controlled by the details of the
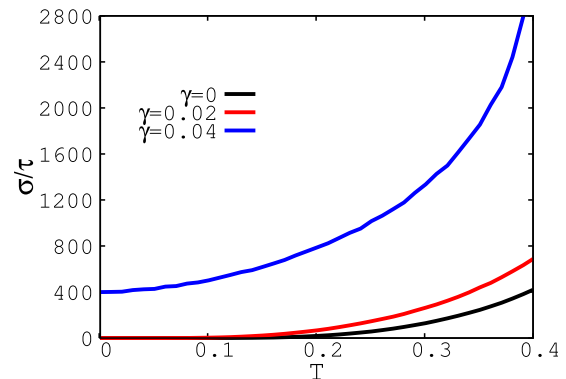

FIG. 9. Resistance for the 10 nm thick film as a function of temperature showing the variation of the minimum as the magnetic field is increased. The lines are fits with Eq. (3).

J_ID: JAP   DOI: 10.1063/1.4846757   Date: 7-December-13   Stage: Page: 7   Total Pages: 8

PROOF COPY [JR13-7386R1] 030348JAP

000000-7   Osquiguil *et al.*   J. Appl. Phys. **114**, 000000 (2013)

electronic structure of the system, details that are far beyond the scope for the simple model presented in Sec. III. Here, the important aspect to be considered is that all these effects are small and the observed low temperature magnetoresistance is positive.

In summary, we have shown that the minimum of the resistivity in thin Cr films is consistent with a simple picture that considers an imperfect nesting in the FS producing a gapless state. The consequent temperature dependence of the effective number of carriers in combination with a reasonable proposition for the relaxation time allows to account for the experimental results quite satisfactorily. We believe that our model is advantageous in the sense that it does not depend on a particular kind of impurity (magnetic, non-magnetic, with bond-states at the Fermi level, defects, vacancies), and thus, it can be useful to understand the low temperature behaviour of the resistivity of a great variety of systems containing spin or charge density waves.

ACKNOWLEDGMENTS

[1]A. W. Overhauser, Phys. Rev. **128**, 1437 (1962).
[2]E. Fawcett, Rev. Mod. Phys. **60**, 209 (1988).
AQ5 [3]E. E. Semenenko, Zh. Eksperim. Teor. Fiz. **11**, 443 (1966) [JETP Lett. **11**, 291 (1966)].
[4]M. N. Coleman and K. W. H. Stevens, Proc. Phys. Soc. London **74**, 390 (1959).
[5]N. S. Rajan, R. M. Waterstrat, and P. A. Beck, J. Appl. Phys. **31**, 731 (1960).
[6]S. Arajs and G. R. Dunmyre, J. Appl. Phys. **37**, 1017, (1966).
[7]S. Arajs, G. R. Dunmyre, and S. J. Dechter, Phys. Rev. **154**, 448 (1967).
[8]B. A. Volkov and V. V. Tugushev, Fiz. Tverd. (Leningrad) **26**, 1428 (1984) [Sov. Phys. Solid State **26**, 1471 (1984)].
[9]V. Galkin, J. Magn. Magn. Mater. **79**, 327 (1989).
[10]V. Yu. Galkin, V. V. Tugushev, and T. E. Tugusheva, Fiz. Tverd. Tela (Leningrad) **28**, 2290–2298 (1986) [Sov. Phys. Solid State **28**(8), ■ (1986)]. AQ4
[11]E. Fawcett and V. Yu. Galkin, J. Magn. Magn. Mater. **104–107**, 759–760 (1992).
[12]E. Fawcett, H. L. Alberts, V. Yu Galkin, D. R. Noakes, and J. V. Jakhmi, Rev. Mod. Phys. **66**, 25 (1994).
[13]E. E. Fullerton *et al.*, Phys. Rev. Lett. **77**, 1382 (1996).
[14]P. Bödeker *et al.*, Phys. Rev. Lett. **81**, 914 (1998).
[15]H. Zabel, J. Phys.: Condens. Matter **11**, 9303 (1999).
[16]R. S. Fishman and Z.-P. Shi, Phys. Rev. B **59**, 13849 (1999).
[17]R. S. Fishman, J. Phys. Condens. Matter **13**, R235 (2001).
[18]K. Mibu *et al.*, Phys. Rev. Lett. **89**, 287202-1 (2002).
[19]E. E. Fullerton *et al.*, Phys. Rev. Lett. **91**, 237201-1 (2003).
[20]D. W. Cooke, Z. Boekelheide, D. R. Queen, and F. Hellman, J. Appl. Phys. **105**, 07C314, (2009).
[21]Z. Boekelheide, D. W. Cooke, E. Helgren, and F. Hellman, Phys. Rev. B **80**, 134426 (2009).
[22]R. K. Kummamuru and Y.-A. Soh, Nature (London) **452**, 859 (2008).
[23]E. Osquiguil, E. E. Kaul, L. Tosi, and C. A. Balseiro, Phys. Rev. B **85**, 104410 (2012).
[24]L. Tosi, E. Osquiguil, E. E. Kaul, and C. A. Balseiro, Europhys. Lett. **100**, 67005 (2012).
[25]J. Kondo, Prog. Theor. Phys. **32**, 37 (1964).
[26]P. W. Anderson, Phys. Rev. **124**, 41 (1961).
[27]J. M. Ziman, *Electrons and Phonons: The Theory of Transport Phenomena in Solids* (Oxford University Press, 2001).
[28]R. R. Hake, D. H. Leslie, and T. G. Belincourt, Phys. Rev. **127**, 170 (1962).
[29]X. Huang and K. Maki, Phys. Rev. B **42**, 6498 (1990).
[30]B. Dóra, K. Maki, and A. Virosztek, Phys. Rev. B **66**, 165116 (2002).
[31]N. I. Kulikov and E. T. Kulatov, J. Phys. F: Met. Phys. **12**, 2291–2308 (1982).
[32]S. Asano and J. Yamashita, J. Phys. Soc. Jpn. **23**(4), 714 (1967).
[33]I. A. Campbell, Phys. Rev. Lett. **26**, 239–242 (1971).